

1 **CSPAD-140k - a Versatile Detector for LCLS Experiments**

2 Sven Herrmann^a, Sébastien Boutet^b, Brian Duda^a, David Fritz^b, Gunther Haller^a, Philip Hart^a, Ryan Herbst^a
3 Christopher Kenney^a, Henrik Lemke^b, Marc Messerschmidt^b, Jack Pines^a, Aymeric Robert^b, Marcin
4 Sikorski^b, Garth Williams^b

5 ^a SLAC National Accelerator Laboratory, Menlo Park, CA 94025, USA

6 ^b LCLS, SLAC National Accelerator Laboratory, Menlo Park, CA 94025, USA

7 corresponding author: Sven Herrmann, herrmann@slac.stanford.edu, tel: +1 650 926-2983

8 SLAC National Accelerator Laboratory, 2575 Sand Hill Road, MS-94, Menlo Park, CA 94025, USA

9 potential referees:

10 Rainer Richter, rar@hll.mpg.de (MPI for physics, Munich, Germany)

11 Bernd Schmitt, bernd.schmitt@psi.ch, (Paul Scherrer Institut, Villigen, Switzerland)

12 Peter Siddons, siddons@bnl.gov, (Brookhaven National Lab, USA)

13

14 **Abstract**

15 With the successful operation of three 2.3 megapixel, 120Hz readout rate, hybrid pixel array detectors
16 at the Linac Coherent Light Source (LCLS), the SLAC National Accelerator Laboratory detector group is
17 now exploring additional applications based on the same detector platform. These megapixel cameras
18 are based on the Cornell-SLAC hybrid Pixel Array Detector (CSPAD).

19 The CSPAD platform is developed around the CSPAD ASIC, a 36 kilopixel device, each pixel at
20 $110 \times 110 \mu\text{m}^2$. Important characteristics of the CSPAD (room temperature operation, 14bit on chip
21 digitization with a purely digital data interface, and scaling modularity) make it an effective choice for
22 designing detector variants that are optimized for a range of experiments and applications.

23 One of the first spin-off detectors based on this proven CSPAD platform is the CSPAD-140k: a 140
24 kilopixel detector, with an active area of approximately $4 \times 4 \text{cm}^2$ and four ASICs, bundled in a small,
25 inexpensive and easy-to-deploy package. Due to its versatility it has already been used successfully in
26 several experiments at the CXI, XPP and XCS instruments at LCLS. The work also describes problems
27 faced by scaling from a prototype system to a full size x-ray camera and presents the current status on
28 the improvements achieved.

29

30 Keywords: hybrid pixel detector; free electron laser; electronics; ASIC; CSPAD;

31 **Introduction**

32 With the successful operation of three 2.3 megapixel, 120Hz readout rate, hybrid pixel array detectors
33 at the Linac Coherent Light Source (LCLS), the SLAC National Accelerator Laboratory detector group is
34 now exploring additional applications based on the same detector platform. These megapixel cameras
35 are based on the Cornell-SLAC hybrid Pixel Array Detector (CSPAD) [1][2][3], particularly the hybrid pixel
36 detector ASIC. This ASIC, with 194×185 pixels of $110 \times 110 \mu\text{m}^2$ size, is the central component of the
37 CSPAD platform. Two ASICs, bump bonded to a single $500 \mu\text{m}$ -thick high-resistivity silicon pixel array
38 sensor, constitute a 2×1 module, which is the basic building block of all CSPAD cameras. The first
39 detector variant based on this proven platform, the CSPAD-140k, uses two of these blocks, glued to a
40 carrier, building up a 2×2 module with a total of about 140 kilopixels. The CSPAD-140k (Figure 1) is a 140
41 kilopixel detector, with an active area of approximately $4 \times 4 \text{cm}^2$, bundled in a small, low-cost and easy-

42 to-deploy package, suitable for various synchrotron and FEL applications. Development and
43 performance optimization of this detector will be discussed in the following paragraphs.

44 (Figure 1 here; caption: The CSPAD 140k detector, an evolution of the pixel array detectors used
45 successfully with megapixel cameras at LCLS.)

46

47 **Electronics and ASIC**

48 The pixel architecture is shown in Figure 2. It consists of a charge sensitive amplifier with two gain
49 settings for collecting the detected signal. The sample and hold stage captures the amplifier output
50 voltage and stores it for digitization. A comparator triggers when an externally supplied ramp falls below
51 the stored signal voltage. A counter counts the clock cycles from the ramp start to the time point when
52 the comparator fires. This implements a single slope analog to digital (A/D) converter. The counter
53 values of all pixels are then readout one after the other.

54 (Figure 2 here; caption: Circuit diagram for a single CSPAD pixel. Functional elements in this circuit are
55 described in the text.)

56 Basic parameters of the CSPAD ASIC are summarized in Table 1 and [1][2][3].

57	pixel size	110 μ m x 110 μ m
58	ASIC size	185 x 194 pixels
59	frame rate	120Hz
60	effective noise	300e- in HG; 1000e- in LG
61	single 8keV Photon SNR	7 in HG; 2 in LG
62	maximum photon count	350 in HG; 2700 in LG

63 [Table 1; caption: Basic physical and performance parameters of the CSPAD ASIC. (HG: high gain, LG: low
64 gain mode)]

65 The first measurements performed at LCLS with a large 2.3 megapixel camera revealed that the single
66 photon gain is smaller than expected from simulations and measurements with the prototype system. A
67 comparison is shown in Figure 3. (Figure 3 here; caption: Comparison of a Monte Carlo simulated pixel
68 histogram and a measured histogram. The Monte Carlo simulation used the CSPADs design parameters.
69 The measurement was performed with an early 2.3 megapixel CSPAD version. The histogram shows the
70 noise peak and the single 8keV photon peak. The measured gain for small signals is 4 times smaller than
71 expected.) Further studies with these cameras showed complex crosstalk behavior between the pixels,
72 partially due to on-chip and partially due to chip-PC-board-system interaction. The CSPAD-140k is
73 especially suited for debugging these effects, as the 2x2 module with 4 ASICs is considerably simpler
74 than the 2.3 megapixel cameras with 64 ASICs, while still using similar electronics and power cycling
75 features. The electronics used in the CSPAD-140k are also much more easily accessible for probing or
76 making modifications.

77 Figure 4 shows the measured ramp function with and without the ASIC. It can be seen that the firing of
78 all the comparators within a short time modifies the external ramp signal. The modified ramp shows an
79 undershoot, which accelerates the firing of comparators that have not yet reached their firing level.
80 (Figure 4 here; caption: Screenshot of the ramp measured with and without the ASICs. The difference
81 between the two ramp functions is shown in the lower trace with a fivefold magnification of the
82 amplitude. The ramp exhibits undershoot when most of the comparators fire and the counters stop

83 counting.) Another aspect of this inter-pixel crosstalk is the modification of the ASIC bias voltages. Figure
84 5 shows the four external bias nodes during the A/D conversion process. (Figure 5 here; caption:
85 Screenshot of the ASIC bias nodes during the A/D conversion process. When most pixels stop counting
86 the comparator bias nodes exhibit undershoot.) When most of the comparators fire, the bias voltage
87 nodes of the comparators exhibit undershoot. This undershoot increases the effective bias current in
88 the comparators, which in turn makes the comparators faster and therefore fire earlier, increasing the
89 correlation of comparator firing. This effect is amplified by the on-board circuitry that is needed for
90 power cycling the LCLS 2.3 megapixel CSPAD cameras: in order to switch the biases on and off at a rate
91 of 120Hz, the nodes cannot simply be tied to a constant voltage. The local power regulators, which have
92 to serve up to 16 ASICs, cannot respond fast enough to sudden changes in supply current when many
93 counters stop clocking. In the current compact camera design, the impulse response on the power
94 nodes feeds through to the ramp generation circuitry.

95 The small signal gain of a pixel depends on the actual ramp steepness the pixel sees around its pedestal
96 value, and therefore on the comparator firing time. Figure 6 shows the measured variation of the gain
97 of a pixel plotted against its average pedestal value (Figure 6 here; caption: Measured variation of the
98 gain of a CSPAD pixel plotted against its average pedestal value. After the first pixel comparators fire the
99 gain breaks down and most pixels show a small gain. Pixels with comparators which fire late show
100 almost nominal gain). It can be seen that the majority of the pixels exhibit a smaller gain for small
101 signals. This apparent smaller gain also affects the measured noise. In contrast, large signals will show
102 the real gain. Furthermore, a camera showing the above effects can exhibit large signal crosstalk when
103 areas of an ASIC are heavily illuminated, resulting in pedestal changes of the non-illuminated regions. As
104 designed, the comparators in illuminated pixels fire later; therefore, their crosstalk contribution is
105 missing at the time the comparators of the non-illuminated pixels fire. Due to this sequence, the
106 comparators in the non-illuminated regions will fire on average a bit later, resulting in an unexpected
107 increase of their digital pedestal value.

108 Modifications in the PCB power supply and improved bias and ramp generation have helped mitigate
109 pixel crosstalk, and the new resulting cameras show a behavior much closer to the expected
110 performance. As an example of the improved performance, Figure 7 shows a single photon histogram of
111 copper fluorescence from a typical pixel measured with the CSPAD-140k. (Figure 7 here; caption:
112 Measured histogram of a CSPAD-140k pixel illuminated with copper fluorescence in high gain mode.)

113 **CSPAD-140k: camera and applications at LCLS**

114 The pulsed nature of the LCLS allows using very short integration times. The CSPAD's hybrid pixel design
115 enables electronic shuttering with signal integration times in the microsecond range; therefore, the
116 detector can operate at room temperature without performance degradation from leakage current. For
117 operation in vacuum, the temperature is stabilized by water cooling. For applications which need longer
118 integration times, like experiments at synchrotrons, the design also supports utilization of a Peltier
119 element to cool the detector. Figure 1 shows the basic elements of the CSPAD-140k camera. The camera
120 housing, which includes the detector-ASIC hybrid and support electronics, is approximately 23.6cm long,
121 4.4cm wide and 4.8cm tall. Behind a black kapton window is a 2x2 module with approximately 4cm x
122 4cm active area and about 140 kilopixels. The CSPAD-140k module uses a fiber-optic interface to
123 transfer data to the data acquisition system. Power and trigger signals are routed via a 26pin DSUB
124 connector. The result is a small but robust interface which enables convenient deployment of the
125 detector in an experiment chamber.

126 A variant designed with slight modification to the package has been built for installation at the MEC
127 instrument, where it will be used as a suitable alternate detector capable of 120Hz readout, replacing a
128 slow CCD camera in a Thomson spectrometer setup. Figure 8 shows a drawing of the MEC spectrometer
129 with the CSPAD-140k (Figure 8; caption: View of a CSPAD-140k integrated as detector of a spectrometer
130 in which will be used by the MEC instrument at LCLS).

131 A major advantage of the small and modular design of the CSPAD-140k is the capability to deploy
132 multiple detectors in various mechanical arrangements. An interesting application of multiple CSPAD-
133 140k modules is to tile them into an arc-like configuration in order to cover a larger angle relative to the
134 interaction point. The multiple single-detector units represent a dedicated compound detector from the
135 data acquisition system point of view. Figure 9 shows the concept for an upcoming experiment at the
136 CXI instrument at LCLS (Figure 9; caption: View of an array of CSPAD-140k detectors organized in a
137 compound detector; this design is under consideration for an upcoming experiment using the CXI
138 instrument at LCLS).

139 The CSPAD-140k has already been used successfully in several experiments using the CXI [4], XPP and
140 XCS instruments at LCLS. As an example, Figure 10 shows a single shot small angle scattering image
141 recorded with CSPAD-140k using the XCS instrument. A dried colloidal dispersion was illuminated with
142 unfocused monochromatic beam of 9.48keV energy. The detector was located 7.8m behind the sample.

143 (Figure 10; caption: Single shot image recorded with the CSPAD-140k using the XCS instrument of LCLS.
144 A dried colloidal dispersion is illuminated with the LCLS unfocused beam at 9.48keV energy. The
145 detector was located 7.8m behind the sample).

146 **Conclusions**

147 A small versatile x-ray camera based on the CSPAD platform has been built at SLAC. This system helped
148 to characterize and improve the performance of all CSPAD cameras. In addition the CSPAD-140k has
149 already been used for several experiments at LCLS and many more applications for this detector at
150 synchrotrons and FELs are expected.

151

152 **Acknowledgements**

153 This work is supported by the Department of Energy, Laboratory Directed Research and Development
154 funding, under contract DE-AC02-76SF00515. Portions of this research were carried out at the Linac
155 Coherent Light Source, a National User Facility operated by Stanford University on behalf of the U.S.
156 Department of Energy (DOE), Office of Basic Energy Sciences (OBES)

157

158 **References**

159 [1] L.J. Koerner, H.T. Philipp, M.S. Hromalik, M.W. Tate, S.M. Gruner, X-ray tests of a Pixel Array Detector
160 for coherent x-ray imaging at the Linac Coherent Light Source, J Instrum, 4 (2009).

161 [2] H.T. Philipp, M. Hromalik, M. Tate, L. Koerner, S.M. Gruner, Pixel array detector for X-ray free
162 electron laser experiments, Nucl Instrum Meth A, 649 (2011) 67-69.

163 [3] L.J. Koerner, M.S. Hromalik, M.W. Tate, S.M. Gruner, Femtosecond Radiation Experiment Detector
164 for X-Ray Free-Electron Laser (XFEL) Coherent X-Ray Imaging, IEEE Transactions on Nuclear Science, 57
165 (2010) 5p.

166 [4] R. Alonso-Mori et al, Shot-by-Shot Energy-Dispersive X-ray Emission Spectroscopy Using an X-ray Free
167 Electron Laser. Submitted for publication.

Figure 1
[Click here to download high resolution image](#)

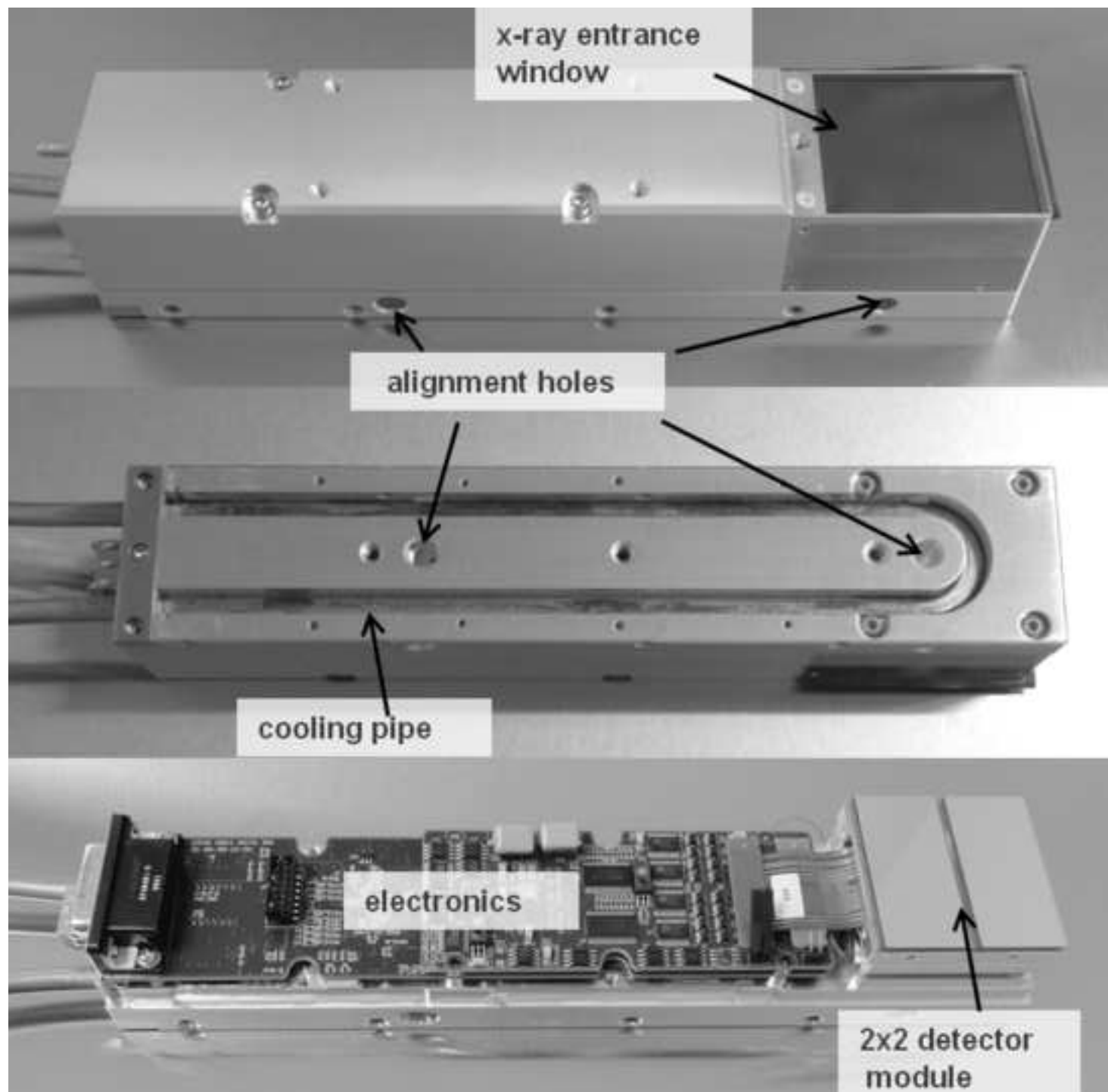


Figure 2
[Click here to download high resolution image](#)

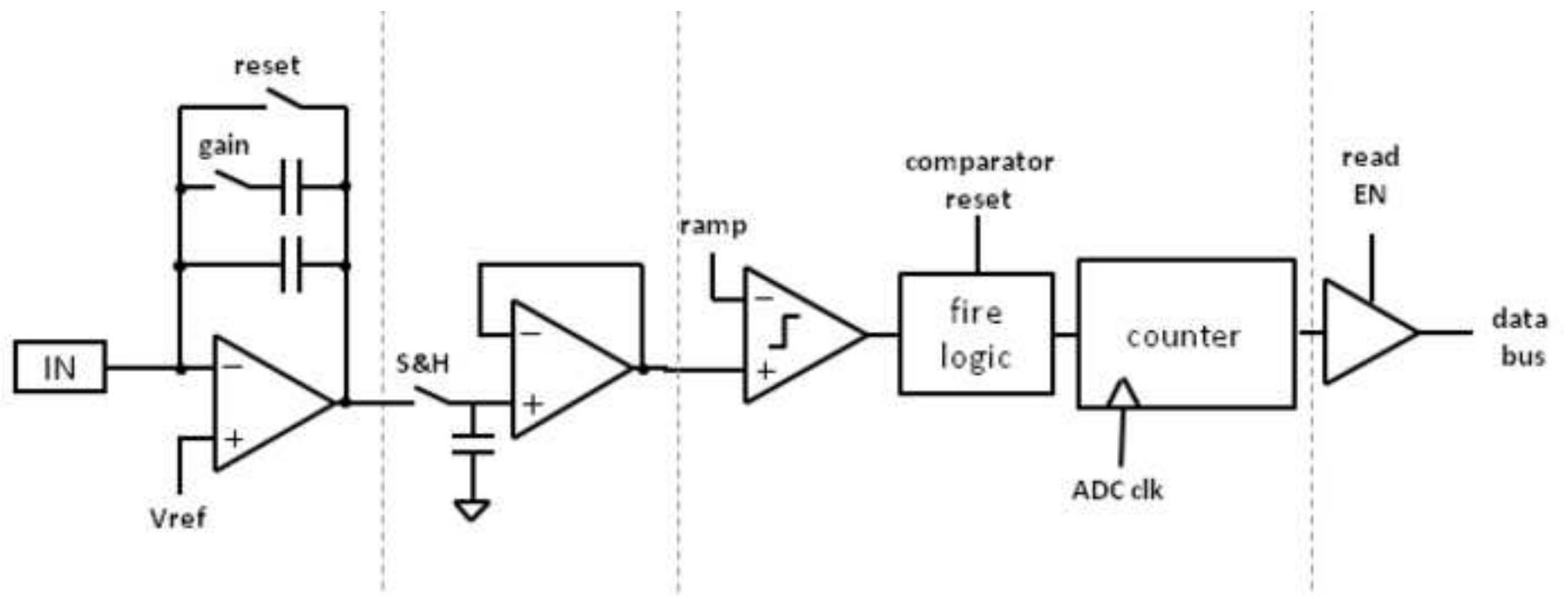


Figure 3
[Click here to download high resolution image](#)

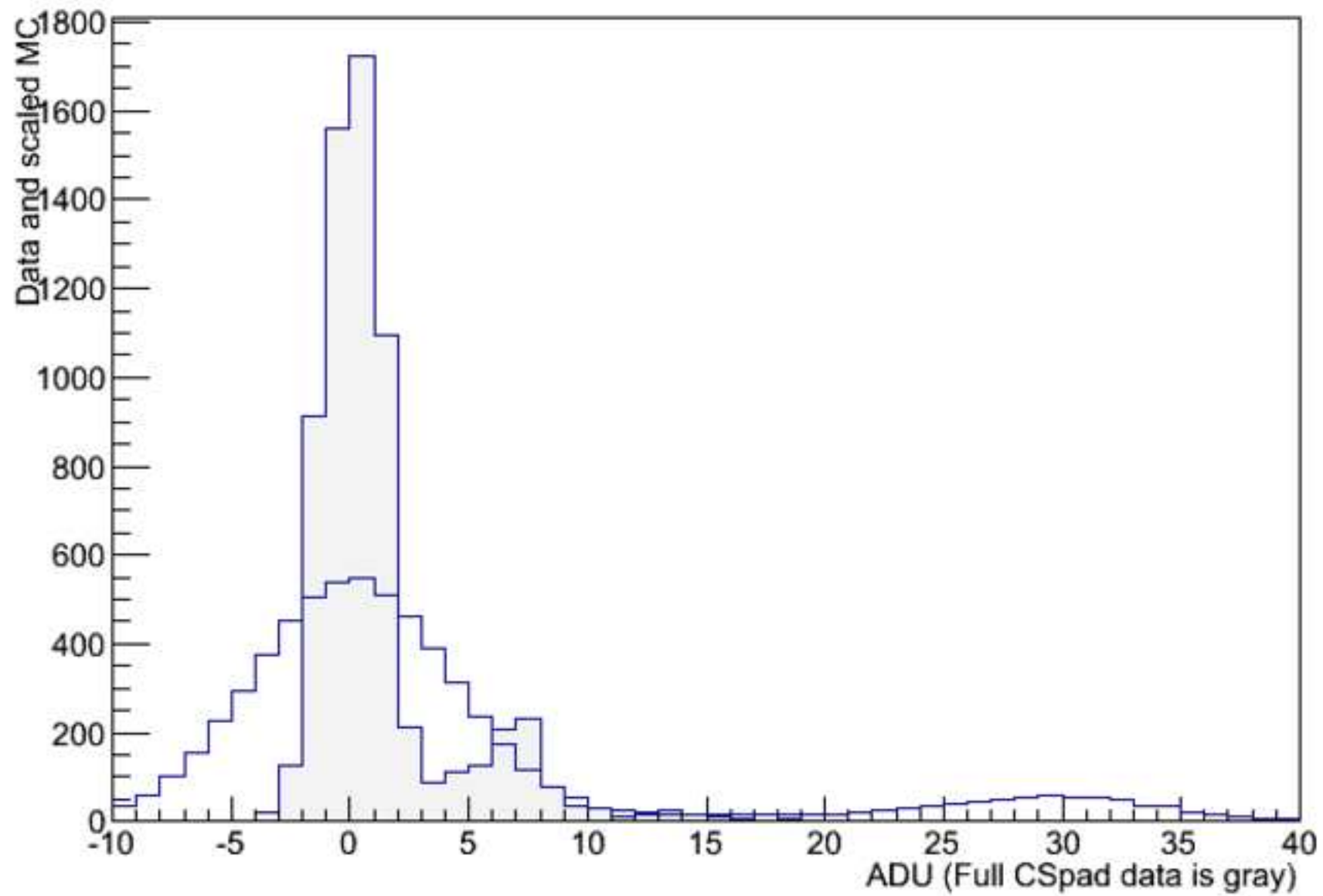


Figure 4
[Click here to download high resolution image](#)

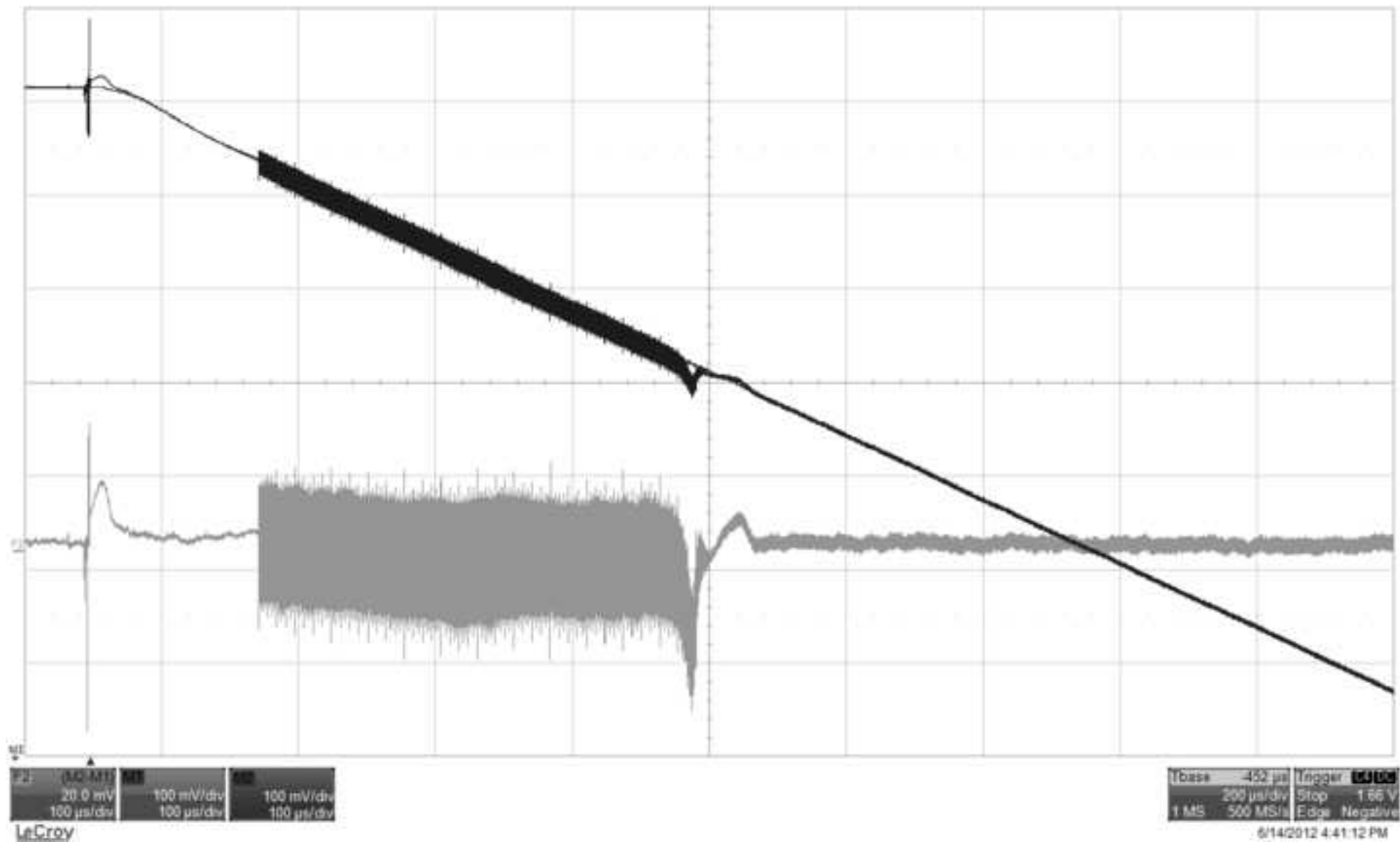


Figure 5
[Click here to download high resolution image](#)

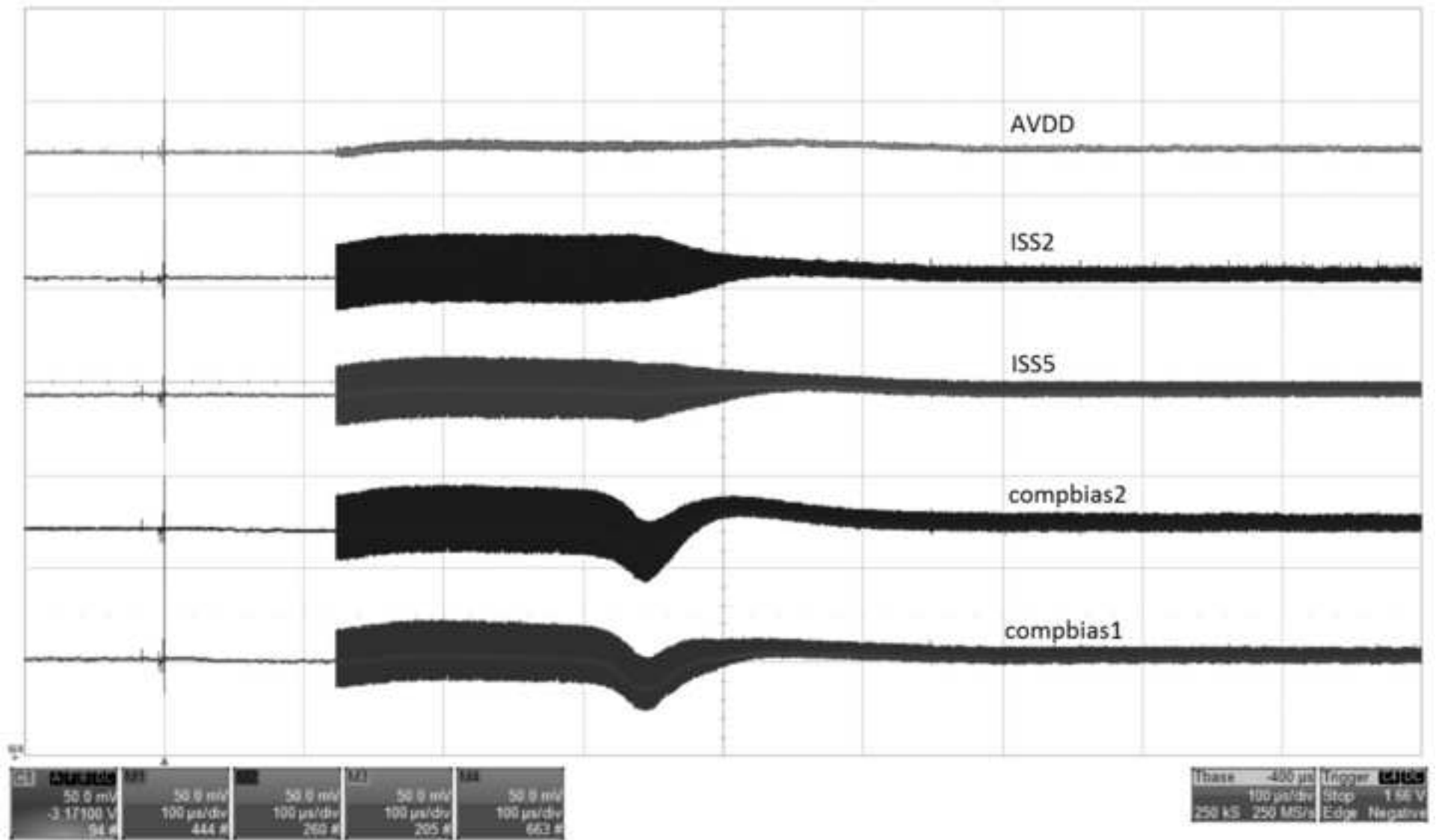


Figure 6
[Click here to download high resolution image](#)

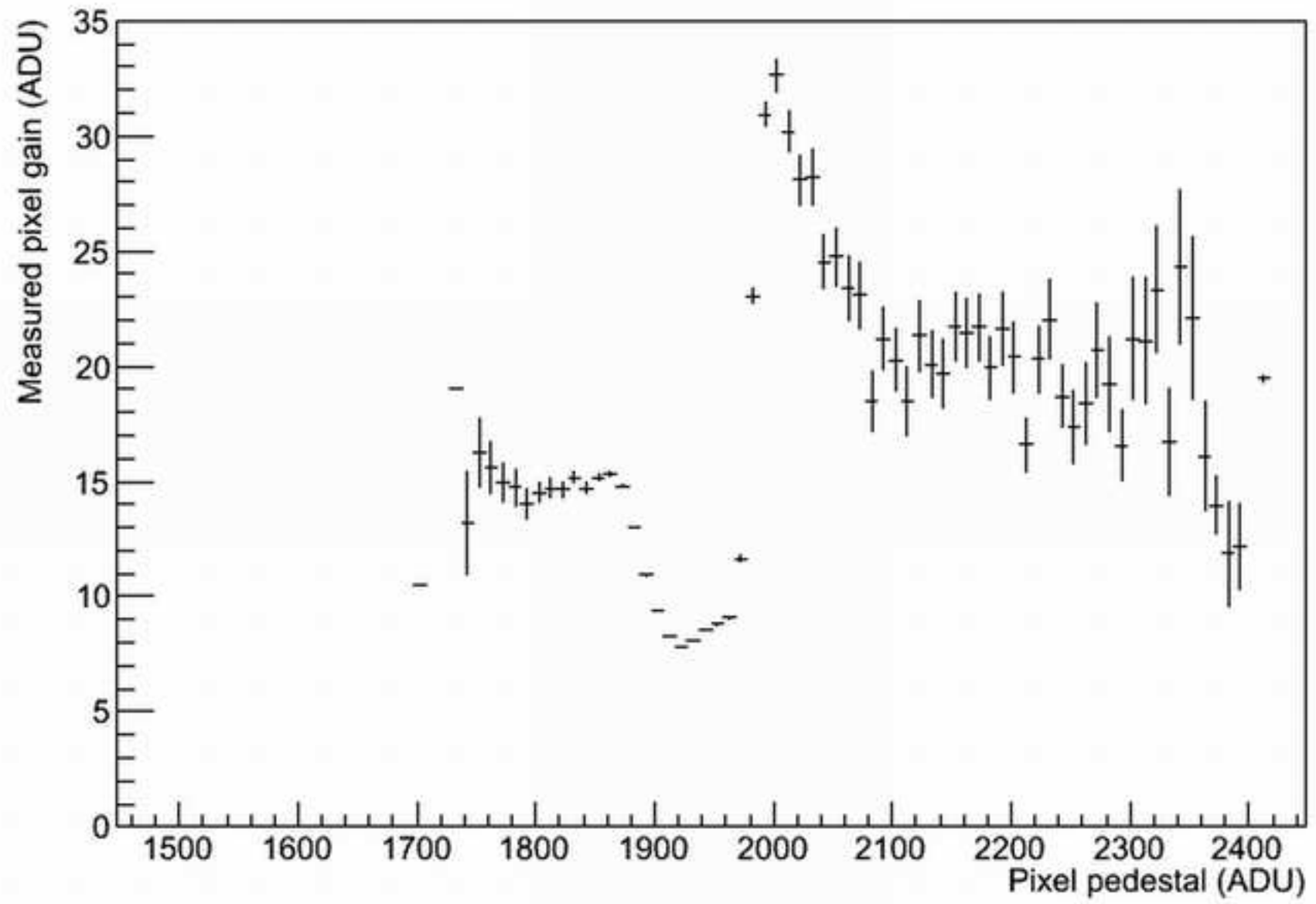


Figure 7
[Click here to download high resolution image](#)

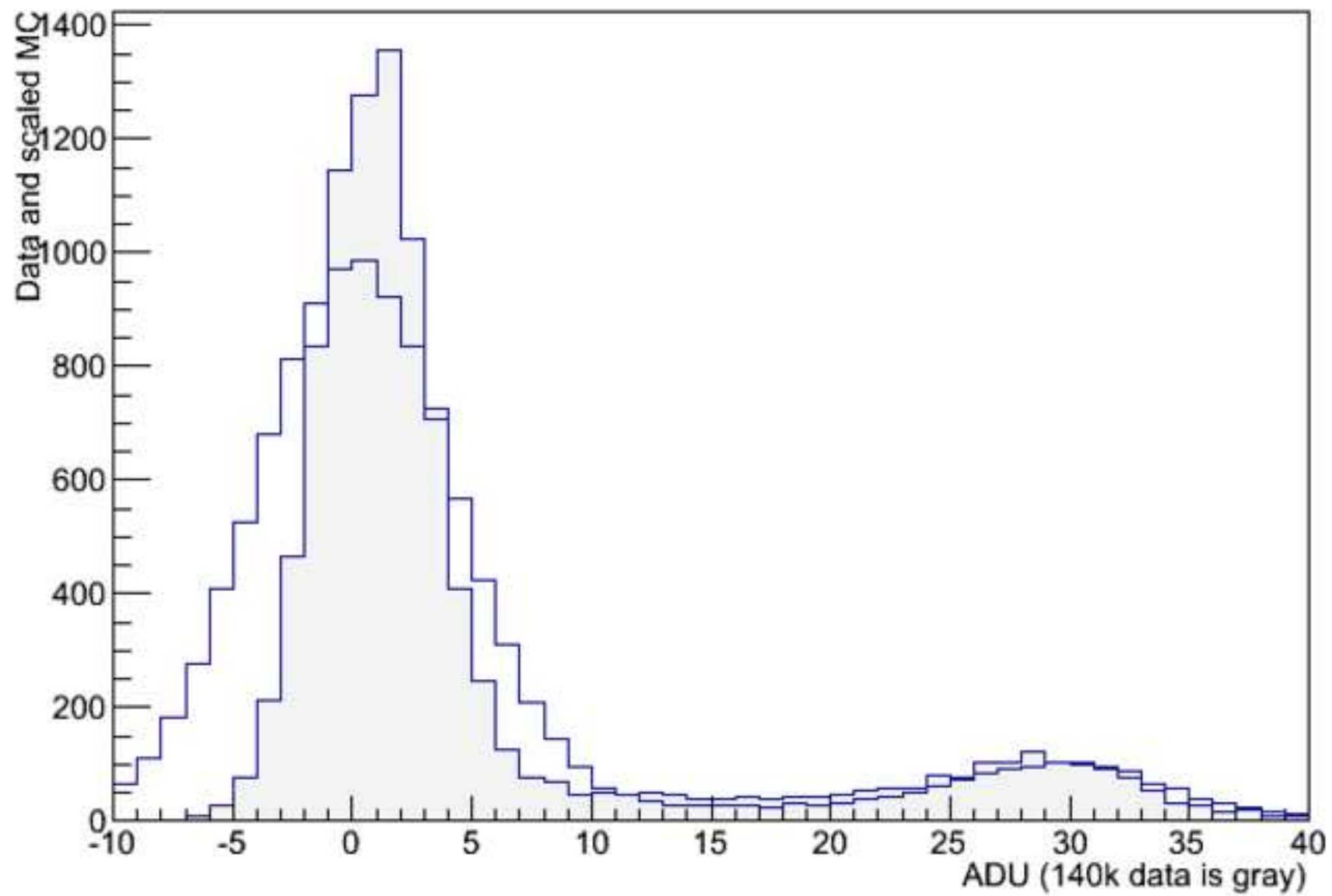


Figure 8
[Click here to download high resolution image](#)

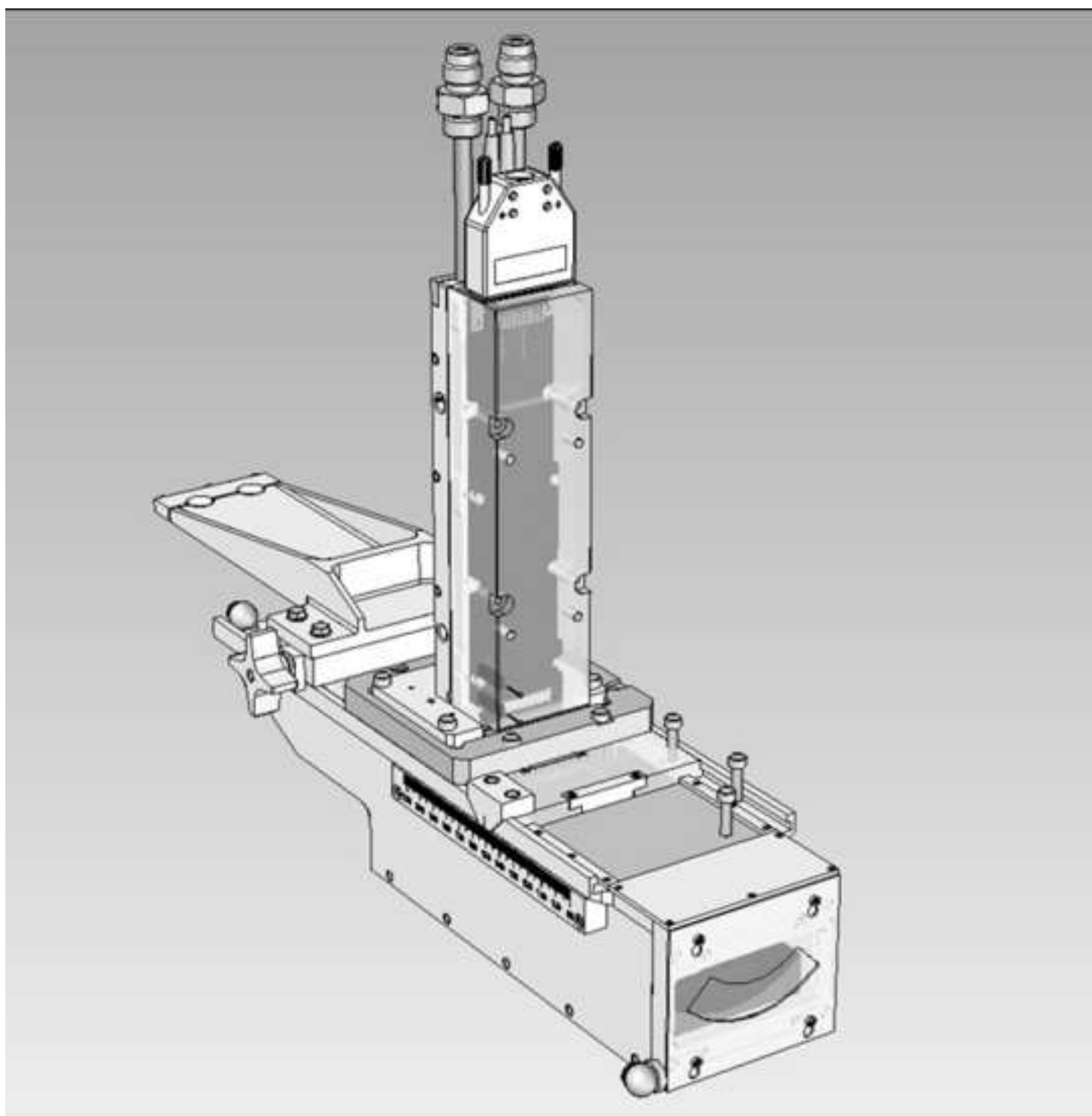


Figure 9
[Click here to download high resolution image](#)

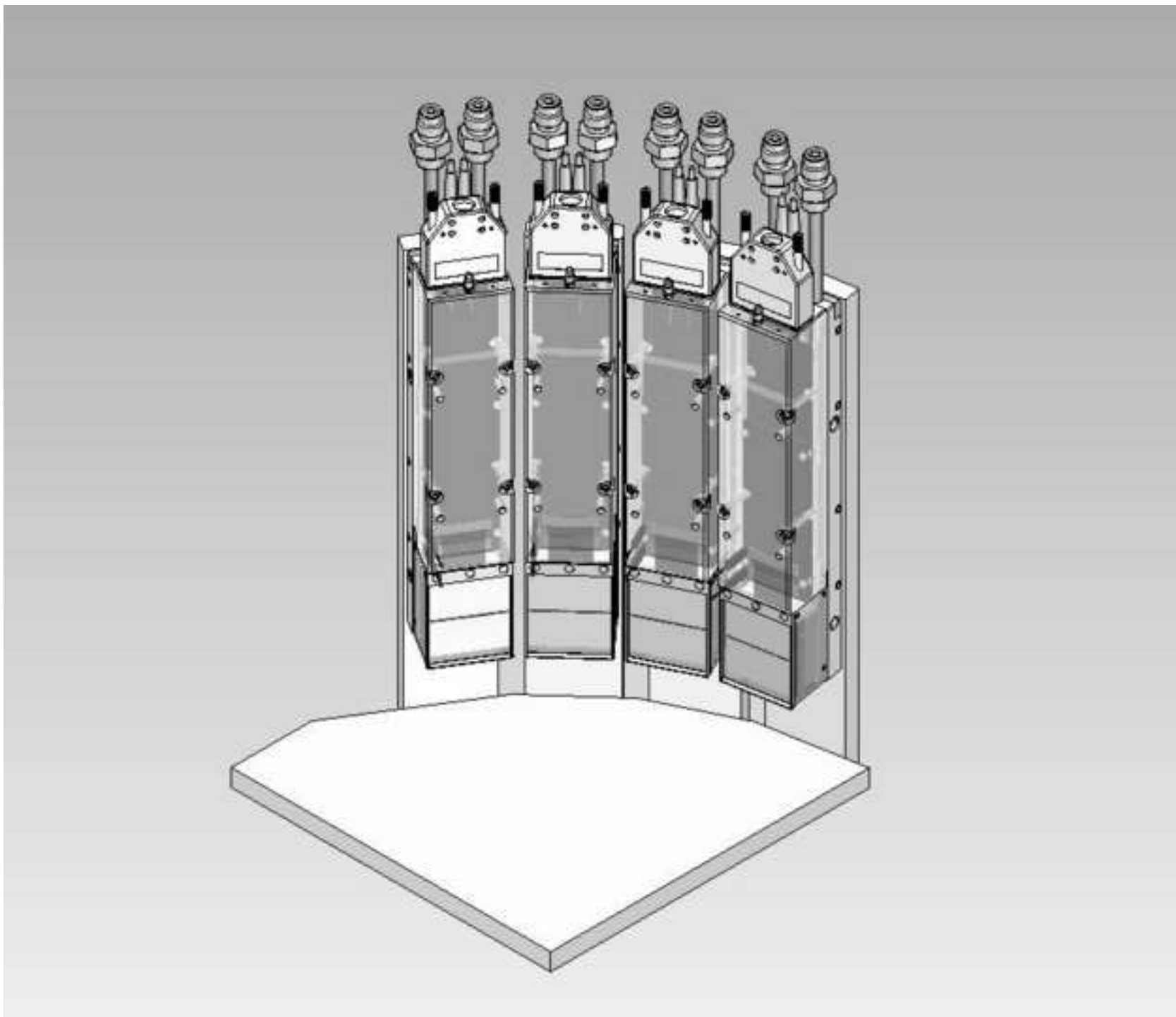


Figure 10 (color)

[Click here to download high resolution image](#)

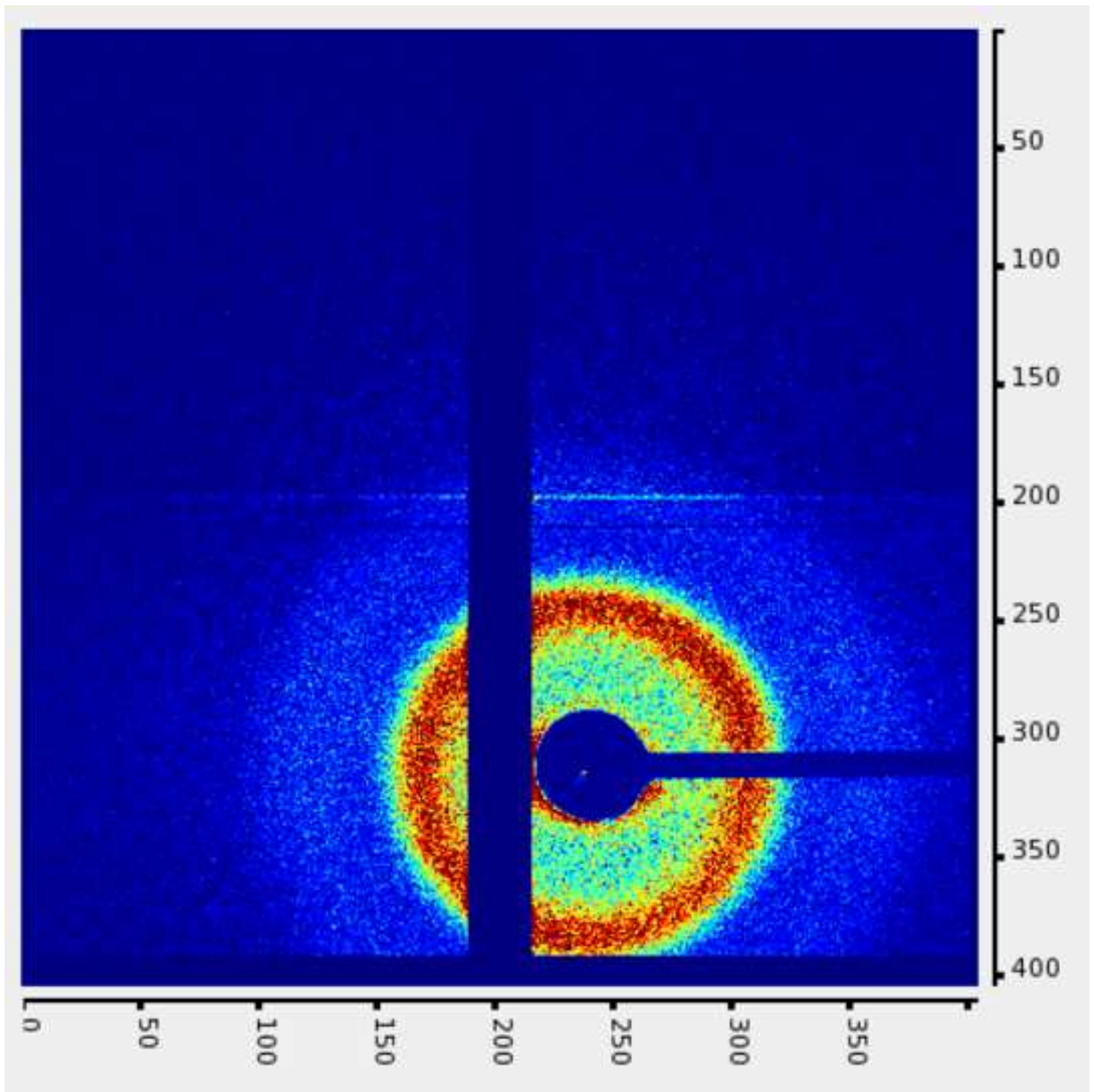


Figure 10 (greyscale)
[Click here to download high resolution image](#)

